

# Preparation and characterization of $(K_{0.5}Na_{0.5})NbO_3$ ceramics

Hansu Birol\*, Dragan Damjanovic, Nava Setter

*Ecole Polytechnique Fédérale de Lausanne (EPFL), Laboratoire de Céramique (LC), CH-1015 Lausanne, Switzerland*

Received 25 June 2004; received in revised form 17 November 2004; accepted 26 November 2004

Available online 21 January 2005

## Abstract

In this paper the preparation and characterization of the ceramic material  $(K_{0.5}Na_{0.5})NbO_3$  (KNN) has been studied. Although conventional processing of KNN is often reported to result in sintered bodies lacking sufficient density, samples produced in this work exhibit theoretical density over 95% and yield superior piezoelectric properties than those obtained by the same method and reported previously. The electromechanical coupling coefficient in the thickness direction,  $k_t$ , is found to reach 45%. Apart from  $k_t$ , the piezoelectric coefficients in longitudinal and planar directions ( $d_{33}$  of 100pC/N and  $d_{31}$  of 43pC/N), hysteresis loop, pyroelectric coefficient measurements and dielectric properties are presented.

© 2004 Elsevier Ltd. All rights reserved.

**Keywords:** Sintering; Dielectric properties; Piezoelectric properties; Perovskites;  $(K, Na)NbO_3$

## 1. Introduction

Potassium sodium niobate  $(K_{1-x},Na_x)NbO_3$  ceramics are reported to show desirable properties for solid ultrasonic delay-line applications and ultrasonic transducers. Its low dielectric constant and high electromechanical coupling coefficient contribute to this.<sup>1,3</sup> A maximum value of radial coupling coefficient,  $k_p$ , is obtained by 50% Na addition to the  $KNbO_3$ .<sup>1</sup> This composition is reported to be composed of a virtual morphotropic phase boundary, where the total polarization can be maximized due to increased possibility of domain orientation.<sup>2</sup> Exact crystallographic nature of this boundary in KNN is presently not well understood and it may be different than the one in lead-zirconate titanate solid solution.

However, a major problem concerning this material is reported to be difficulty in obtaining samples with a high density by conventional preparation and sintering.<sup>2–5</sup> A deviation from stoichiometry resulting in the formation of extra

phases, a relatively low sintering temperature compared to other piezoelectric materials, and the difficulty of obtaining a fine microstructure during sintering are some of the factors which make the densification of KNN ceramics difficult. An alternative solution for this problem has been the use of hot pressing pursued by many researchers.<sup>4,5</sup> Although this method yields high densities and better properties compared to conventional air-sintered KNN, it still needs careful investigation and optimization of sintering parameters to result in reproducible and high quality ceramics. Additionally, it is a more expensive route compared to conventional sintering. The goal of this work has been to produce KNN samples by conventional air sintering in attempt to reach high densities and characterize the material.

## 2. Preparation of samples

Pure grades of  $K_2CO_3$ ,  $Na_2CO_3$  and  $Nb_2O_5$  powders (>99.95%) were used as initial materials. The use of two different powders with carbonate origin requires extra care to be taken against humidity. Thermo gravimetric analysis (TGA) shows that the powders lose weight up to 180 °C, which is equivalent to the water absorbed. Therefore, in order to obtain the stoichiometric material composition

\* Corresponding author. Present address: Ecole Polytechnique Fédérale de Lausanne (EPFL), Laboratoire de Production Microtechnique (LPM), CH-1015 Lausanne, Switzerland. Tel.: +41 21 693 77 58; fax: +41 21 693 38 91.

E-mail address: [hansu.birol@epfl.ch](mailto:hansu.birol@epfl.ch) (H. Birol).

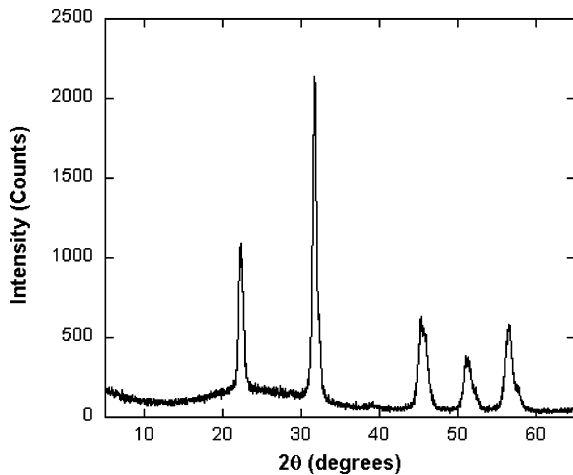


Fig. 1. X-ray pattern of calcined powder.

all powders were separately dried in an oven at 220 °C for 4 h prior to mixing. The stoichiometric amounts were transferred to a 200 ml plastic jar, which was previously filled with 5 mm diameter zirconia grinding balls and 40 ml of acetone. The total amount of milled powder was 20 g. The batch was ball-milled at 97 rpm for 24 h. At the end of the milling, the slurry was dried and kept in an oven at 120 °C.

Calcination was performed in an alumina crucible that was heated to 120 °C before the transfer of the dried powder. After the transfer of the powder, it was heated at a rate of 3 °C/min to 825 °C and kept at that temperature for 4 h. The cooling rate was 10 °C/min. The X-ray pattern of a calcined powder obtained by this method is given in Fig. 1.

Pellets of 7 mm diameter were uniaxially pressed at 25 MPa and sintered at 1114 °C for 2 h with a heating rate of 5 °C/min and cooling rate of 10 °C/min in oxygen rich atmosphere, which yielded relative density up to 95–96% (the-

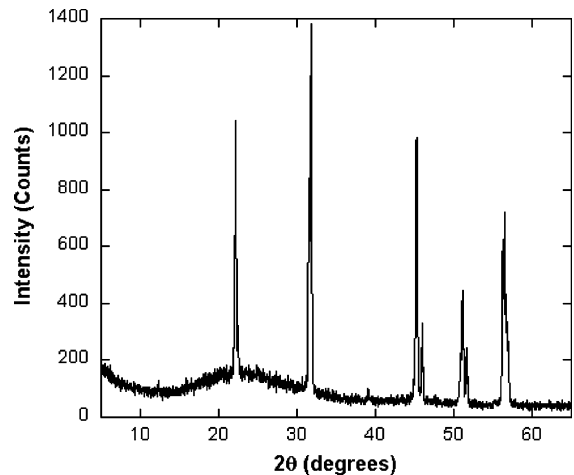


Fig. 2. X-ray pattern of a sintered KNN sample.

oretical density is 4.51 g/cm<sup>3</sup>).<sup>5</sup> Densities were measured by Archimede's technique. An X-ray pattern and SEM image of a sample prepared by this method is given in Figs. 2 and 3.

XRD patterns of both the calcined powder and the sintered pellet are in agreement with the expected orthorhombic phase. Shoulders on the right hand side of the powder X-ray pattern could be linked to slight off-stoichiometry. These additional features disappear in sintered samples.

### 3. Characterization

The samples were prepared in varying aspect ratios for different measurements. The aspect ratio selected for resonance measurement was around 10 as required by IEEE standard,<sup>6</sup> for quasistatic measurements of the longitudinal piezoelectric coefficient,  $d_{33}$ , around 3–4<sup>7</sup> and for hysteresis and dielectric measurements around 14 to minimize electric field. The

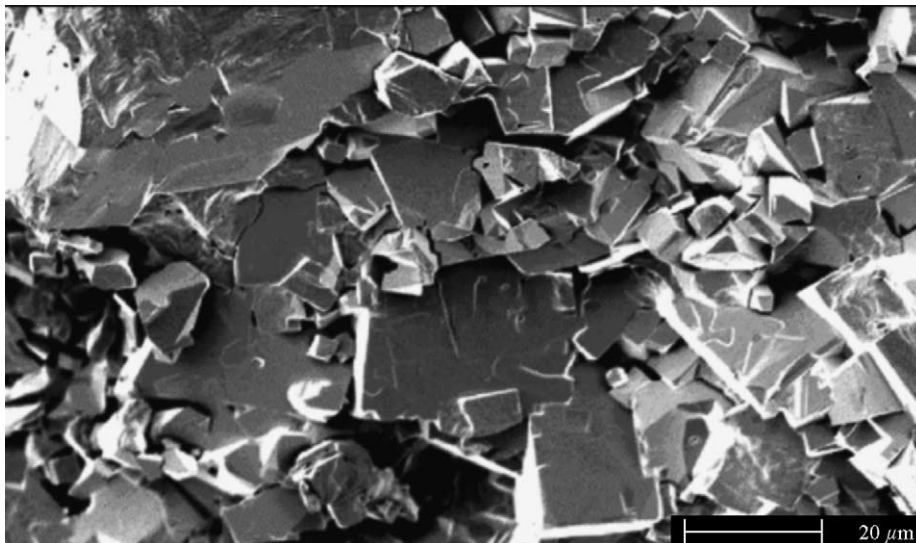


Fig. 3. Fractured surface of a sintered KNN sample.

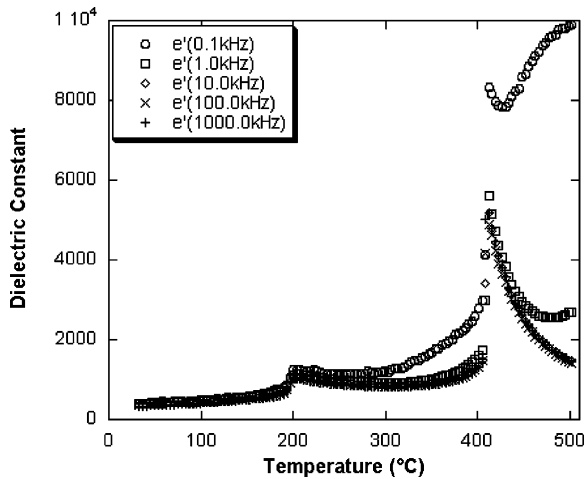


Fig. 4. Temperature vs. dielectric constant.

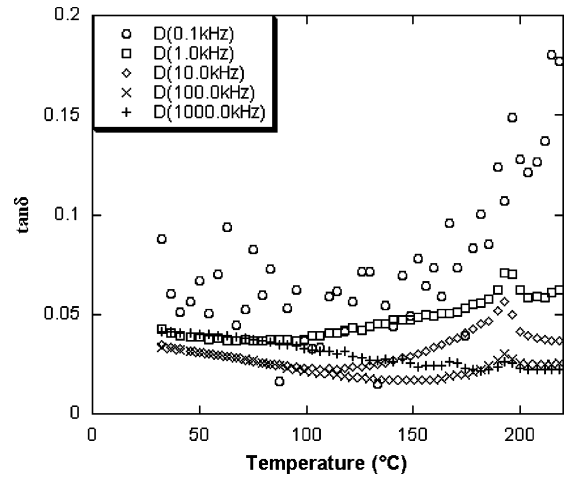


Fig. 6.  $\tan \delta$  vs. temperature up to 220 °C. (The inconsistent data at the lowest frequency is due to the noise.)

largest surfaces of the samples were electroded with gold for electrical characterization measurements.

### 3.1. Dielectric constant versus temperature

Dielectric constant versus temperature data was recorded at five frequencies from  $10^2$  to  $10^6$  Hz using HP 4282A-LCR bridge. The information on dielectric constant and losses are presented in Figs. 4 and 5. Fig. 6 shows the losses up to 230 °C. The material possesses two maximums in dielectric values around 400 and 190 °C, each representing the cubic to tetragonal and tetragonal to orthorhombic phase transitions, respectively.

Low frequency dispersion can be observed above 200 °C and it might be linked to hygroscopic sensitivity of the material.<sup>8</sup> Formation of a hydroxide at the material surface, can well lead to such additional loss mechanism. This behavior is also seen in most of the KNN samples, prepared by hot forging with relative densities reaching close to 100%.

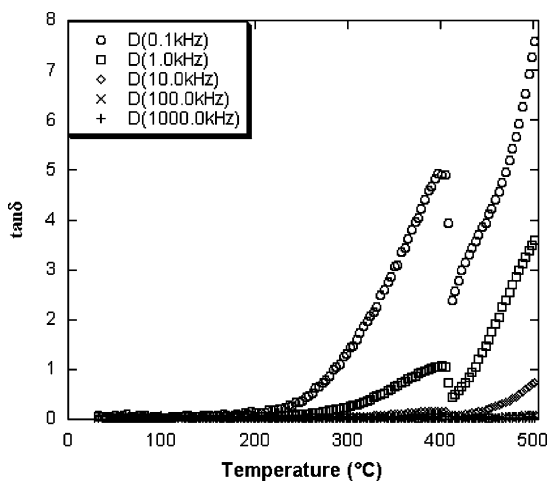


Fig. 5.  $\tan \delta$  vs. temperature. (There is no maximum for losses at 100 and 1000 kHz around 400 °C.)

### 3.2. Polarization versus electric field

Polarization versus field behavior was investigated at room temperature (Fig. 7). At maximum field, the coercive field,  $E_c$ , has a value of 20 kV/cm and the remanent polarization is 0.20 C/m<sup>2</sup>. Loop pinching is observed at lower fields, which is linked to a preferred orientation of defect dipoles in the material. At fields higher than 50 kV/cm, pinching vanishes and well formed symmetric hysteresis loops are observed.

### 3.3. Poling and resonance measurements

The electric field was applied through the thickness direction of the electroded pellets. The samples were heated over the tetragonal to orthorhombic phase transition temperature, which is around 200 °C, and cooled down to room temperature under 15 kV/cm of electric field.

In order to get the maximum polarization, different parameters were investigated such as effect of electric field,

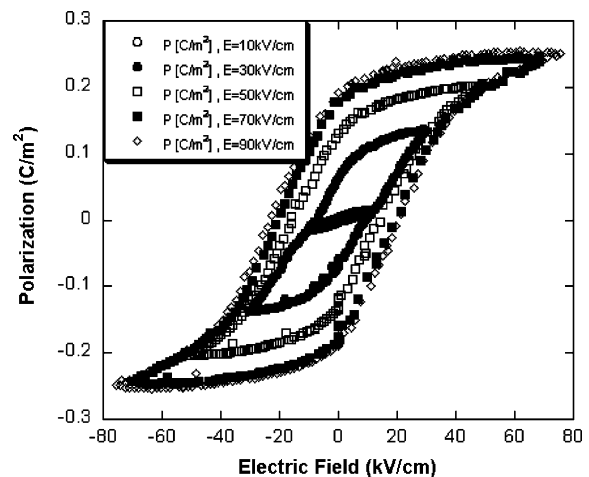


Fig. 7. Hysteresis loops at room temperature.

Table 1  
Results of the resonance measurements

$\epsilon_{33}/\epsilon_0$	472
$\sigma_{12}$	0.33
$S_{11}$ (m <sup>2</sup> /kg)	$8.7 \times 10^{-12}$
$d_{31}$ (pC/N)	43.4
$k_{31}$	0.23
$k_p$	0.39
$k_t$	0.45

time and temperature. It is observed that best properties are obtained (Table 1) using the technique<sup>1</sup> described above.

Resonance measurements were carried out with HP 4194A LCR-meter. The poled sample was connected to the bridge carefully not to create any stresses on it. All the properties were calculated from the equation of admittance for a disc-shaped sample (thickness mode coupling coefficient from<sup>6</sup>).

### 3.4. Longitudinal $d_{33}$ measurements

The longitudinal piezoelectric charge coefficient was measured under a sinusoidal AC pressure field. The AC pressure range was from 1.5 to 6.5 MPa. The details of experimental procedure are described elsewhere.<sup>9</sup> The frequency dependence of the piezoelectric coefficient was examined under a DC pressure of 16 MPa. Fig. 8 shows data for a sample, which was poled by field cooling.

The motion of domain walls, which are activated by the applied AC pressure leads to a high value of piezoelectric coefficient apart from intrinsic effect. This is the irreversible contribution and it is originated basically from the ferroelastic nature of the non-180° domain walls. Slowing down of response at high frequencies is seen in a lower value of  $d_{33}$ .

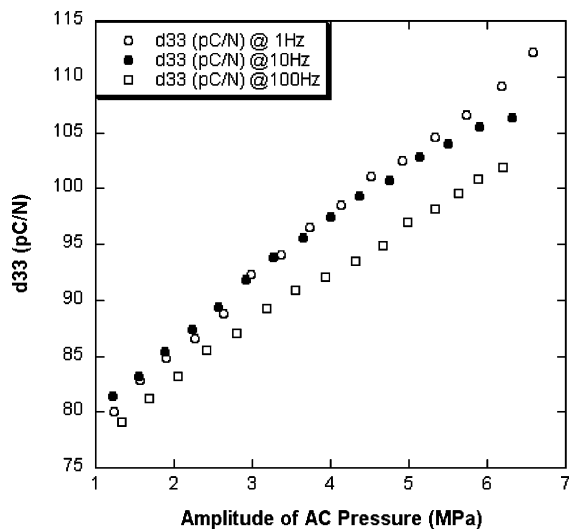


Fig. 8. Longitudinal piezoelectric coefficient,  $d_{33}$ , as a function of the AC pressure.

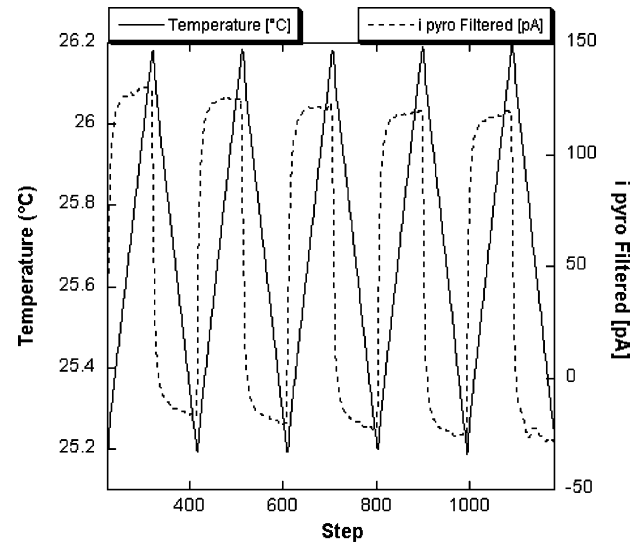


Fig. 9. Material response (rectangles) to changing temperature (triangles) conditions. (I pyro filtered is the pyroelectric current that is created as a result of charge release on the specimen surface due to temperature variations.)

### 3.5. Pyroelectric measurements

Measurements were made using a heat regulator, which has a sensitivity of 0.001 K/step, KH function generator and a HP 3478 A multimeter. Temperature range is selected between 27 and 28 °C as shown in Fig. 9. Pyroelectric effect shows itself as release of charges on the surface of the specimen upon temperature change. These charges are detected as a current that is called pyroelectric current and presented by  $I_p$ . One can see pyroelectric current on the right hand side y-axis of Fig. 9 and the temperature on the left. The average pyroelectric coefficient obtained from this measurement gives a value of 140  $\mu\text{C}/\text{m}^2 \text{K}$ , which is comparable to 83  $\mu\text{C}/\text{m}^2 \text{K}$  of LiNbO<sub>3</sub> single crystal<sup>10</sup> and 110  $\mu\text{C}/\text{m}^2 \text{K}$  of lead germanate<sup>11</sup>.

## 4. Study of aging

The sintered ceramics were observed to have increasing dielectric losses starting from the very initial time of preparation (Fig. 10).

Although it is not completely understood, it is estimated to be linked to humidity sensitivity of these ceramics. We probably have a case of absorption and desorption of humidity on a long time scale. It is important to notice that the dielectric loss at 1 MHz is below 0.05 through the whole time period, which is quite promising for device applications.

In addition to the aging of dielectric loss we conducted another study on aging of electromechanical coupling coefficient in thickness direction,  $k_t$ , which is the figure of merit for ultrasonic transducers operating at high frequencies. Fig. 11 shows the results.

Table 2  
Comparison of properties obtained by different groups

Properties	Air-sintered, Jaeger–Egerton <sup>4</sup> , $K_{0.5}Na_{0.5}NbO_3$	Air-sintered, Kosec <sup>5</sup> , $K_{0.5}Na_{0.5}NbO_3$	Air-sintered, this study, $K_{0.5}Na_{0.5}NbO_3$	Hot-pressed, Jaeger–Egerton <sup>4</sup> , $K_{0.5}Na_{0.5}NbO_3$	Hot-forged Schultze <sup>3</sup> , $K_{0.5}Na_{0.5}NbO_3 + 4 \text{ mol\% Ba}$
$\rho$ ( $10^3 \text{ kg/m}^3$ )	4.25	4.20	4.30	4.46	4.28
%TD	94.24	93.13	95.3	98.89	94.90
$d_{33}$ (pC/N)	80		110	160	115
$d_{31}$ (pC/N)	32		43.4	49	
$k_p$	0.36	0.23	0.39	0.45	0.37
$k_t$			0.45		
$k_{31}$	0.22		0.23	0.27	
$\sigma_{12}$	0.27 (assumed)		0.33	0.27 (assumed)	

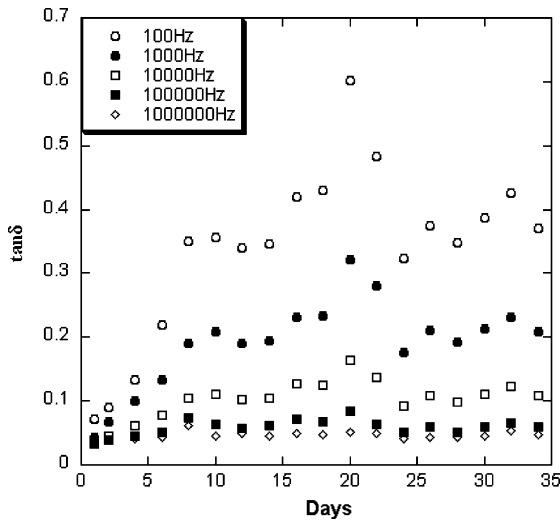


Fig. 10. Aging of dielectric loss in virgin sample.

At this point it is important to understand whether the observed decrease comes from a possible humidity effect or relaxation of domain walls. In order to approach this problem, a sample was put into oven at  $100^\circ\text{C}$  for 3 h after which the dielectric losses and  $k_t$  was checked. It was observed that the former dropped below 0.05 at all frequencies whereas, the

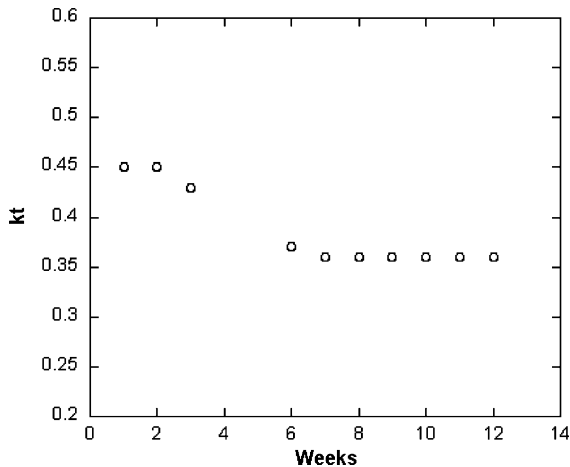


Fig. 11. Aging of the thickness coupling coefficient,  $k_t$ , in a KNN ceramic.

latter remained constant. So, it can be concluded that this drop from 0.45 to 0.36 in 12 weeks seems to be result of domain wall relaxation process.

## 5. Discussions

A comparison of properties, which are obtained by different processing routes of different groups regarding  $(K_{0.5}Na_{0.5})NbO_3$  ceramic is shown in Table 2.

Properties of ceramics produced in this study using conventional sintering are comparable to hot forged/pressed ones. High piezoelectric coefficients and coupling coefficients demonstrate this fact. According to our observations high properties are related to keeping material free of humidity and as close to stoichiometry as possible.

## 6. Conclusions

An intensive study on processing and properties of KNN ceramic using conventional powder synthesis was conducted. Some of the interesting aspects related to processing and properties can be summarized as in the following:

1. The processing of KNN needs extreme control of many parameters starting from initial powder characteristics till sintering atmosphere.
2. The aging of properties (dielectric loss,  $k_t$ ) is observed. It is seen that dielectric losses decrease after heating the samples in oven at  $100^\circ\text{C}$ .
3. The maximum polarization is obtained by field cooling under an electric field of  $15 \text{ kV/cm}$ , which is applied starting from the tetragonal to orthorhombic transition temperature.
4. Excellent electromechanical coupling coefficients both in radial and thickness directions ( $k_p$  of 0.39 and  $k_t$  of 0.45) are reached.

## References

1. Egerton, L. and Dillon, D. M., Piezoelectric and dielectric properties of ceramics in the system potassium-sodium niobate. *J. Am. Ceram. Soc.*, 1959, **42**, 438–442.

2. Jaffe, B., Cook, W. R. and Jaffe, H., *Piezoelectric Ceramics*. Academic Press Limited, Bedford, Ohio, 1971, p. 193.
3. Ahn, Z. S. and Schulze, W. A., Conventionally sintered  $(\text{Na}_{0.5}\text{K}_{0.5})\text{NbO}_3$  with barium additions. *Commun. Am. Ceram. Soc.*, 1987, **70**, C18–C21.
4. Jaeger, R. E. and Egerton, L., Hot pressing of potassium-sodium niobates. *J. Am. Ceram. Soc.*, 1962, **45**, 209–213.
5. Kosec, M. and Kolar, D., On activated sintering and electrical properties of  $\text{NaKNbO}_3$ . *Mater. Res. Bull.*, 1975, **10**, 335–340.
6. IEEE Standard on Piezoelectricity. *IEEE T. Ultrason. Ferr.*, 1996, **43**, 719–722.
7. Barzegar, A., Damjanovic, D. and Setter, N., The effect of boundary conditions and sample aspect ratio on apparent  $d_{33}$  piezoelectric coefficient determined by direct quasistatic method. *IEEE Trans. UFFC*, 2004, **51**, 262–270.
8. Sundarakannan, B., Kakimoto, K. and Ohsato, H., Frequency and temperature dependent dielectric and conductivity behavior of  $\text{KNbO}_3$  ceramics. *J. Appl. Phys.*, 2003, **94**, 5182–5187.
9. Damjanovic, D., Demartin, M., Shulman, H. S., Testorf, M. and Setter, N., Instabilities in the piezoelectric properties of ferroelectric ceramics. *Sens. Actuators A-Phys.*, 1996, **53**, 353–360.
10. Byer, L. and Roundy, C. B., Pyroelectric coefficient direct measurement technique and application to a nsec response time detector. *Ferroelectrics*, 1972, **3**, 333–338.
11. Whatmore, R. W., Pyroelectric devices and materials. *Rep. Prog. Phys.*, 1986, **49**, 1335–1386.